博 士 論 文

Effect of Silver Diamine Fluoride on Bonding Performance and Ultra-morphological Characteristics to Sound Dentin
(フッ化銀ジアミンの健全象牙質に対する接着性と超微細形態特性への影響について)

令和６年３月申請

北海道大学
大学院歯学院口腔医学専攻

パピチャヤ　インタジャック
Papichaya Intajak

1. Introduction

Dental caries is a multifactorial disease that localized the dissolved inorganic structure of dental hard tissue [1]. Effectively delaying and preventing tooth decay is crucial in maintaining healthy teeth, clinicians and researchers are increasingly using technologies and medications to accomplish the concept of minimally invasive restorative. One notable innovation is silver diamine fluoride (SDF), which was first introduced in the 1970s based on its arrest of dental caries [2, 3]. SDF or $Ag(NH_3)_2$ F consists of approximately 253,870 ppm silver, 44,880 ppm fluoride, and amine as a solvent. SDF showed superior performance over fluoride vanish alone in terms of effectiveness on caries arrest and safety [4, 5]. Unlike other fluoride products, SDF contains both fluoride and silver. The interaction of fluoride ions with calcium and phosphate produces fluorohydroxyapatite, which reduces the solubility of the mineral [6]. Furthermore, silver was proven to have an antimicrobial effect [7-9]. Subsequently, in 2014, the Food and Drug Administration (FDA) approved SDF to be used as a tooth desensitizer [10]. All of the above, SDF has been continuously used for arresting caries [11-14], caries prevention [5, 15, 16], cavity cleanser [17], tooth desensitizer [18-21], root canal irrigant [22], and newly introduced to use as caries detector due to the darkening effect on caries-affected dentin [23].

During application for caries arrest, SDF could inevitably contaminate sound dentin surfaces. Previous studies have shown that there was no adverse effect of SDF contamination on adhesive-dentin bond performance in self-etch mode (SE) and etch-and-rinse mode (ER) to sound dentin of permanent [24, 25] and primary teeth [26]. However, the bond strength of SDF on sound dentin is affected by various factors such as SDF application technique [27], concentration and duration of SDF application [25, 28], the type of application modes of adhesive [29], and the type of adhesives and restorations [17, 30, 31].

The newest type of adhesive called universal adhesive has been developed, which can be used in a variety of cases in clinical settings and it is simple to use. This adhesive has improved the bond durability of bonding [32, 33] and can be applied with SE, ER, and selective enamel etching mode which exhibited a different bonding mechanism to the substrates [33]. However, it is still unclear whether the application of SDF affects the dentin bonding performance of universal adhesives and no study has been conducted on the ultra-morphological characteristic changes in sound dentin after bonding with them. Therefore, this study aimed to evaluate the microtensile bond strength (μTBS) of SDF-contaminated sound dentin to different universal adhesives, and ultra-morphological characteristic changes induced by SDF. The null hypotheses were; (1) there were no effects of SDF on the bond strength of adhesives to sound dentin, (2) there were no effects of the application modes of adhesive on the bond strength of SDF-contaminated dentin, and (3) there were no difference in the bond strengths among adhesives.

2. Materials and methods

This study was approved by the research ethics committee at Hokkaido University (approval number 2018-7). One hundred fifty-three non-carious human third molars were cleaned with saline, stored in 0.5% chloramine-T solution at 4ºC, and used within 6 months after extraction.

2.1. Specimens preparation and bonding procedures

Ninety-six non-carious human third molars were used for the μTBS test. The teeth were horizontally cut to expose flat mid-coronal dentin using a low-speed diamond saw (Isomet 1000, Buehler, Lake Bluff, IL, USA) under copious water coolant. The dentin surfaces were grounded manually with 600-grit SiC paper (Fujistar, Sankyo Rikagaku Co., Saitama, Japan) under running water for 60 s. Then the teeth were randomly divided into two main groups: (1) with the application of SDF (Saforide, Bee brand Medico Dental, Osaka, Japan) as an SDF-contaminated dentin group and (2) without SDF as a sound dentin group. In the SDF-contaminated dentin group, all the dentin surfaces were applied SDF with agitation for 1 min, then left for 2 min followed by rinsing with distilled water for 30 s. Each group was randomly divided into six subgroups (n = 8 / group) according to different application modes and universal adhesives: SE and ER modes were performed with Scothbond Universal Plus Adhesive (SUP; 3M ESPE, St Paul, MN, USA), G2-Bond Universal Adhesive (G2B; GC Corporation, Tokyo, Japan), and Clearfil Mega Bond 2 (MB2; Kuraray Noritake, Tokyo, Japan). In ER mode, 35% phosphoric acid etchant (Ultradent, South Jordan, UT, USA) was used. Each adhesive was performed following the manufacturer's instruction (Table 1) and light-cured using LED curing light (Pencure 2000, J Morita Corp., Osaka, Japan) with an intensity of 1,500 mW/cm^2. After the application of adhesives, 2 layers of 2-mm-thick resin composite (Clearfil AP-X, Kuraray Noritake) were built up. All the specimens were

stored in distilled water at 37 ºC for 24 h.

Table 1 Materials used in this study.

Materials	Composition	pH	Application
Saforide Lot no. 104TA	38 % $Ag(NH_3)_2F$ (44,800 ppm F)	10	1. Apply with agitation for 1 min. 2. Leave undisturbed for 2 min. 3. Rinse with distilled water for 30 s and gentle air-blow.
Scothchbond Universal Plus Adhesive Lot no. 7610150	10-MDP, HEMA, vitrebond copolymer, filler, ethanol, water, initiators, silane, accelerator, dimethacrylates	2.7	1. Apply the primer with agitation for 20 s. 2. Dry with air-blow at least 5 s. 3. Light-cure for 10 s.
G2-BOND Universal Lot no.2102151	Primer: 4-MET, 10-MDP, 10-MDTP, dimethacrylates, water, acetone, photoinitiators, silica filler Bond: UDMA, dimethacrylate, bis-GMA, photo-initiators, silica filler	1.5	1. Apply the primer and leave undisturbed for 10 s. 2. Dry with moderate air-blow for 5 s. 3. Apply bonding agent and gentle air-blow to create uniform film. 4. Light-cure for 5 s.
Clearfil Mega BOND 2 Lot no. 000140	Primer: 10-MDP, HEMA, Hydrophilic aliphatic dimethacrylate, dl-CQ, accelerators, water, dyes Bond: 10-MDP, Bis-GMA, HEMA, dl-CQ, dimethacrylate, initiators, accelerators, colloidal silica	~2	1. Apply the primer and leave undisturbed for 20 s. 2. Dry with mild air-blow for 5 s. 3. Apply bonding agent and gentle air-blow to create uniform film. 4. Light-cure for 10 s.
Ultra-Etch Lot no. BLK2V	35% Phosphoric acid, glycol, cobalt aluminate blue spinel	< 1	1. Apply for 15 s. 2. Rinse with distilled water for 15 s and gentle air-blow.
Clearfil AP-X Lot no. 1SO150	Bis-GMA, TEGDMA, silanated barium glass filler, silated silica filler, silanated colloidal silica, dl-CQ, initiators, accelerators, pigments		

10-MDP: 10-methacryloyloxydecyl dihydrogen phosphate; HEMA: 2-hydroxyethyl methacrylate; 4-MET: 4-methcryloxyethyl trimellitic anhydride; 10-MDTP: 10-methacryloyloxydecyl dihydrogen thiophosphate; UDMA: urethane dimethacrylate; Bis-GMA: bisphenol A diglycidyl methacrylate; CQ: camphorquinone; TEGDMA: triethylene glycol dimethacrylate.

2.2. μTBS test and fracture modes analysis

After 24 h storage, each bonded specimen was sectioned into beams with a cross-sectional area of approximately 1 × 1 mm^2 using a low-speed diamond saw. The beam was fixed to a Ciucchi's jig with cyanoacrylate glue (Model repair II Blue, Dentsply-Sankin, Otahara, Japan) and subjected to a tensile force at a crosshead speed of 1 mm/min in a desktop testing machine (EZ-S, Shimadzu, Kyoto, Japan) until failure occurred. Bond strength was shown in MPa. The mean bond strength of eleven beams was obtained from each tooth, generating eight values for each tested group [34, 35].

After the μTBS test, the fracture modes of the specimens were visualized by light microscope (x 20 magnification; Magnifier Light, Asone, Osaka, Japan). Then coated with Pt-Pd for 120 s and confirmed by scanning electron microscope (SEM; S-4000, Hitachi, Tokyo, Japan) at an accelerating voltage of 10 kV. The fractured beams were categorized into four fracture modes: cohesive failure in dentin, cohesive failure in composite, adhesive failure, and mixed failure [34].

2.3. Elemental analysis of the fractured specimens by SEM/EDX

After the μTBS test, the dentin side of beams (categorized as adhesive failure) of each group was further prepared for elemental analysis (n = 3). They were immediately fixed overnight in 2.5% glutaraldehyde containing 0.1 M sodium cacodylate buffer. Then rinsed with the same buffer and dehydrated in an ascending concentration series of ethanol. Finally, the dehydrated samples were immersed in hexamethyldisilazane solution for 10 min [36]. The fractured beams were sputter-coated with carbon (15 nm layer thickness), and analyzed in a field emission SEM (FE-SEM; JSM-7200F, JEOL Ltd., Tokyo, Japan) with the operating condition of 15 kV and using energy-dispersive X-ray spectroscopy (EDX; EX-94300S4L1Q, JEOL Ltd.).

2.4. SDF-contaminated dentin surfaces observation by SEM

Nine dentin discs were divided into 3 groups (n = 3) for transverse observation as follows: (1) polished with 600-grit SiC paper for 60 s (2) polished with 600-grit SiC paper for 60 s + SDF 3 min + rinsed with distilled water for 30 s, and (3) following (2) + 35% phosphoric acid 15 s + rinsed with distilled water 15 s. A groove was prepared at the pulpal side of the dentin disc with a regular grit cylinder diamond bur (Diamond point FG, Shofu, Kyoto, Japan). All discs were fixed and dehydrated as previously mentioned. Finally, the discs were carefully fractured along the pre-prepared groove by a scalpel blade and hammer. The morphology of longitudinal fractures was observed under SEM.

2.5. Interfacial observation by SEM

Twenty-four teeth (n = 2) were prepared following the same protocol as for the μTBS test. The specimens were sectioned perpendicularly to the interface to acquire two slabs using a low-speed diamond blade. The slabs were prepared following a protocol described by Yuan et al [37]. After that, all the slabs were sputter coated with Pt-Pd for 120 s and observed under SEM with an accelerating voltage of 10 kV.

2.6. Interfacial observation by TEM and STEM/EDX analysis

Twenty-four teeth (n = 2) were prepared and bonded as previously mentioned for the μTBS test, then restored with a thin layer of flowable resin composite (Omnichroma flow, Tokuyama dental, Tokyo, Japan). After 24 h of water storage, the specimens were trimmed into rectangular blocks approximately 1 × 1 × 2 mm. The blocks were processed for TEM according to the

procedure described by Van Meerbeek et al [38]. The ultra-thin specimens were observed with a transmission electron microscope (TEM; JEM-1400, JEOL, Tokyo, Japan) operating at 80 kV.

Ultra-thin specimens of ER groups were further observed by a scanning transmission electron microscope (STEM; JEM-2010F, JEOL, Tokyo, Japan) at 80 kV, with high-angle annular dark field imaging (HAADF) and EDX for elemental analysis [39].

2.7. Statistical analysis

The μTBS data were analyzed for normal distribution using the Kolmogorov-Smirnov test and homogeneity of variance was tested by Levene's test. According to those test results, a Three-way ANOVA and Duncan test were conducted to analyze μTBS ($\alpha = 0.05$). Statistical analysis was achieved using the SPSS software package, Statistical Package for the Social Sciences for Windows (SPSS version 25; IBM Corp, Armonk, NY, USA).

3. Results

3.1. μTBS test and fracture modes analysis

The results of μTBS are summarized in Fig. 1. There were no pre-test failures in this study. Three-way ANOVA revealed that the type of adhesive used ($F = 15.273$, $p < 0.0001$), application mode ($F = 54.518$, $p < 0.0001$), and application of SDF ($F = 347.580$, $p < 0.0001$) were all individually significant factors. The interaction among the three factors was not statistically significant ($F = 1.731$, $p = 0.183$). Additionally, there was no significant interaction between adhesive and application mode ($p = 0.295$). However, the interactions between SDF and adhesive ($p < 0.001$), and between SDF and application mode ($p = 0.036$) were significant. Significantly lower μTBS was observed when adhesives were bonded to SDF-contaminated dentin compared to sound dentin in all groups. Regarding the application mode of adhesives, ER groups showed a significantly higher μTBS than SE groups in SUP and MB2 for sound dentin, however, G2B revealed no significant difference between ER and SE groups. Whereas ER groups revealed a significantly higher μTBS than SE groups in all adhesives for SDF-contaminated dentin. For sound dentin, no significant difference in all adhesives with ER mode. Meanwhile, in SE mode, G2B demonstrated significantly higher bond strength when compared with SUP.

The percentage of fracture modes analysis is shown in Fig. 2. The most frequent fracture was adhesive failure in all SDF-contaminated dentin groups. In the sound dentin group, fractures were predominantly cohesive failure in dentin and mixed failure. Furthermore, the ER mode exhibited a higher incidence of cohesive in dentin compared to the SE mode in the SUP and MB2 groups.

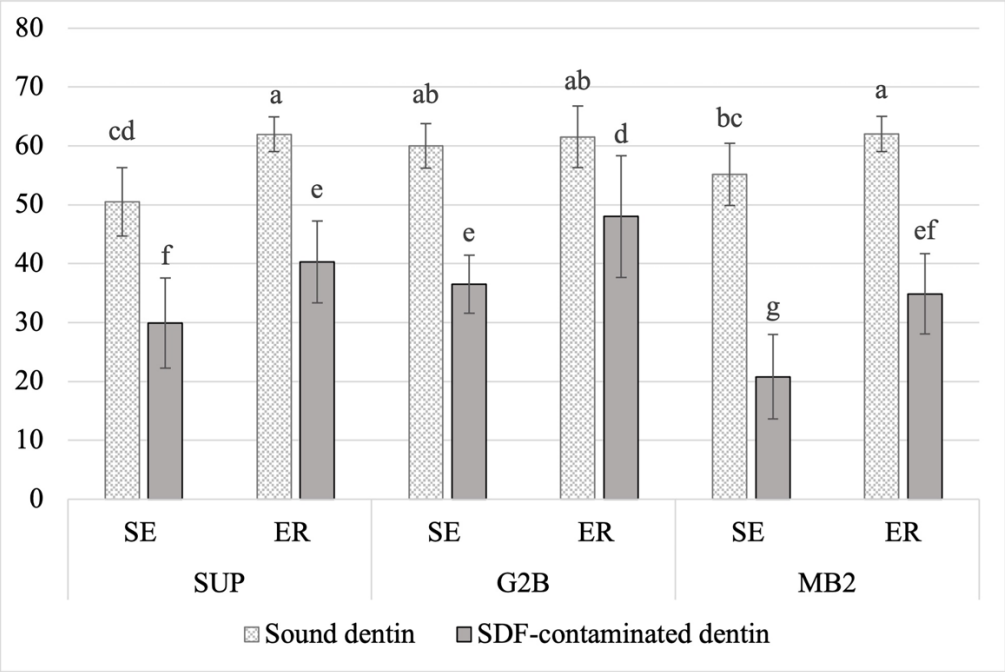

Fig 1. The graph represents the μTBS (in MPa) of all groups. The mean values in each bar with the same lowercase superscript letters are not statistically significantly different.

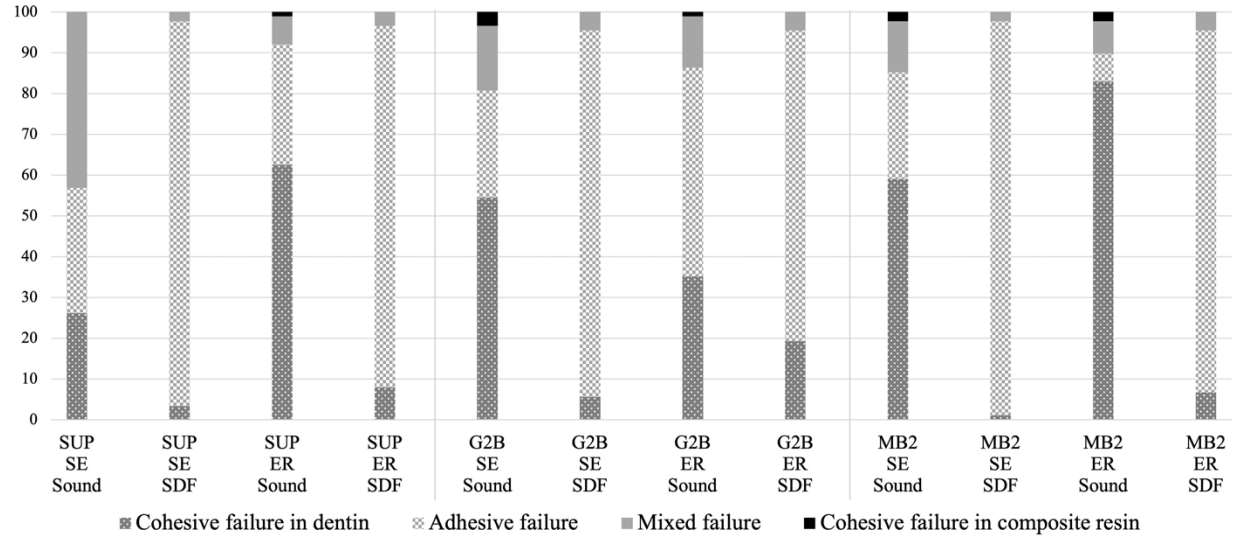

Fig 2. The percentage of failure mode.

3.2. Elemental analysis of the fractured specimens by SEM/EDX

Elemental analysis for the particles that appeared on the fractured surfaces on the dentin side is presented in Fig. 3. Fluoride and silver were not detected in the dentin surfaces of sound dentin groups (Fig. 3a,3b), while SDF-contaminated dentin groups exhibited peaks of fluoride and silver in the EDX spectra (Fig. 3c,3e,3g). Additionally, EDX mapping of SDF-contaminated dentin with SUP (Fig. 3f) and G2B (Fig. 3h) in SE mode revealed that the areas of fluoride (in blue) were mainly distributed on the peritubular dentin, whereas silver (in red) were densely filled in the intratubular tubule. The dentin surfaces with MB2 showed a similar trend to SUP and G2B (data not shown).

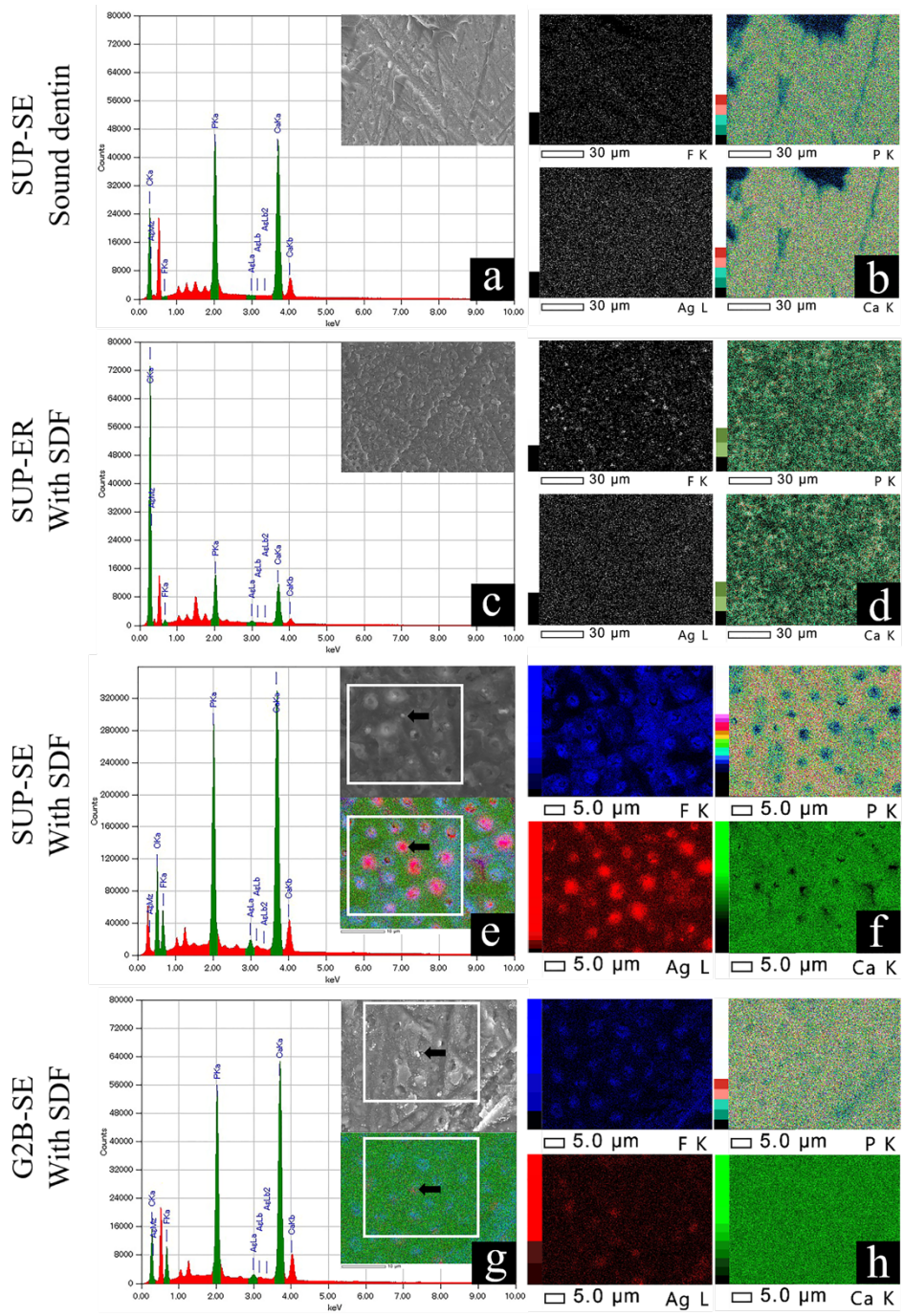

Fig 3. Representative SEM images and corresponding EDX spectra, along with elemental mapping of fluoride (F), silver (Ag), phosphate (P), and calcium (Ca) are presented for the fractured surface of the dentin side of SUP specimens (**a-f**), and G2B (**g-h**). **a-b**: The fractured image of sound dentin bonded with SUP in SE mode, revealing no presence of

silver and fluoride. **c-d**: The fractured images of SDF-contaminated dentin bonded with SUP in ER mode, presenting peaks of silver and fluoride. Fluoride is detected in EDX mapping, while silver does not appear. **e-f**: The fractured surface of SDF-contaminated dentin bonded with SUP in SE mode, revealing peaks of silver and fluoride, along with EDX mapping indicating silver in red, fluoride in blue, and calcium in green. **g-h**: The fractured surface of SDF-contaminated dentin bonded with G2B in SE mode, presenting peaks of silver and fluoride, along with elemental mapping. White box and arrow highlight the same area.

3.3. SDF-contaminated dentin observation by SEM

Longitudinally sectioned of sound dentin and SDF-contaminated dentin are presented in Fig. 4. In the sound dentin group prepared with 600-grit SiC paper, a homogenized smear layer formed on the dentin surface, along with smear plugs within the dentinal tubules (Fig. 4a,4d). In the SDF-contaminated dentin group rinsed with water, a thin smear layer with multiple sizes of angular and globular particles were observed on the top of the dentin surface (Fig. 4b). Moreover, a pack of small globular particles (approximately 0.1 μm) were visible within the dentinal tubule (Fig. 4e). In the SDF-contaminated dentin followed by phosphoric acid etching, multiple sizes of angular and globular particles were also observed on the dentin surface (Fig. 4c). Some small globular particles were observed within the dentinal tubule beneath the demineralized dentin (Fig. 4f), but a lesser amount when compared to the water-rinsing group (Fig. 4e).

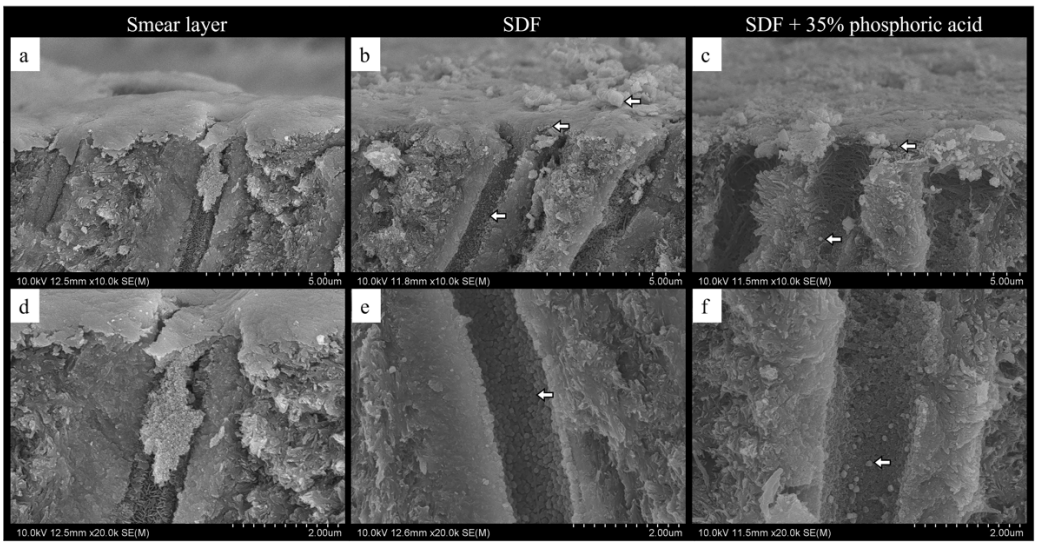

Fig 4. SEM images showing longitudinally sectioned dentinal tubule of sound dentin (**a,d**) and SDF-contaminated dentin (**b-c,e-f**). **a,d**: Dentin after polished with 600-grit SiC paper, forming a homogenized smear layer on the dentin surface and smear plugs within the dentinal tubules, with a higher magnification shown in d. **b,e**: SDF-contaminated dentin followed by water rinsing, presenting remaining particles on top of the dentin surface and within the dentinal tubule, with a higher magnification shown in e. **c,f**: SDF-contaminated dentin followed by 35% phosphoric acid etching, showing demineralized dentin approximately 3 μm with remaining particles on top of the dentin surface and within dentinal tubule below the demineralized dentin, with a higher magnification shown in f. White arrow indicates precipitating particles.

3.4. Interfacial observation by SEM

SEM images of the adhesive-dentin interface are shown in Fig. 5. In the SE mode, abundant cylindrical resin tags were observed in all adhesives when bonded to sound dentin (Fig. 5a, 5c, 5e). On the other hand, when SUP and G2B were applied with SE mode on SDF-contaminated dentin,

resin tags were not formed (Fig. 5g, 5i), and MB2 established only a few resin tags (Fig. 5k). In the ER mode, sound dentin revealed a well-demarcated hybrid layer (2-3 μm) and numerous resin tags with small branches (Fig. 5b, 5d, 5f). Similar characteristics were observed when adhesives bonded to SDF-contaminated dentin with ER mode (Fig. 5h, 5j, 5l).

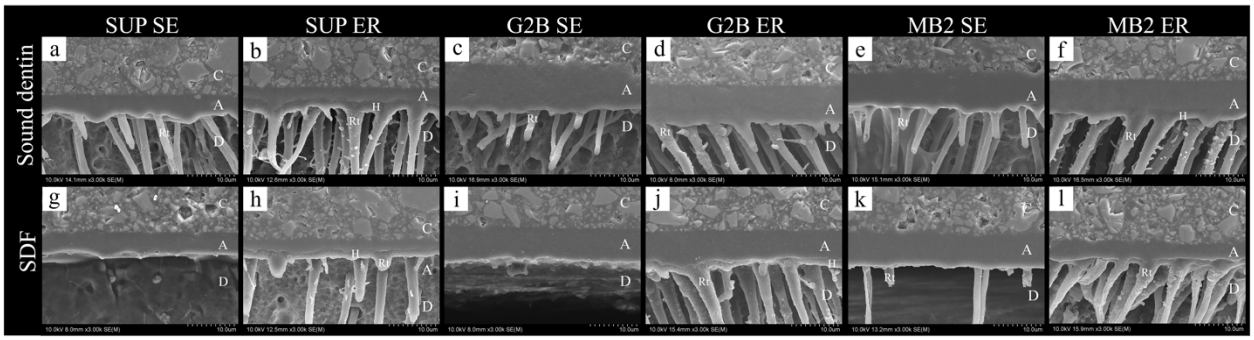

Fig 5. Representative SEM images of the adhesive-dentin interface of each adhesive (x 3,000) on sound dentin (**a-f**) and SDF-contaminated dentin (**g-l**). **a:** SUP with SE mode, revealing intact resin tags with an adhesive layer approximately 5 μm thick. **c,e**: G2B (c) and MB2 (e) with SE mode, presenting intact resin tags with an adhesive layer approximately 10-15 μm thick. **g,i,k**: SDF-contaminated dentin bonded adhesives in SE mode, showing no resin tag in SUP (g) and G2B (i). A few resin tags were observed in MB2 (k). **b,d,f**: Sound dentin bonded adhesives with ER mode, presenting a hybrid layer of approximately 2-3 μm with intact resin tags. **h,j,l**: SDF-contaminated dentin bonded adhesives with ER mode, also revealing a hybrid layer approximately 2-3 μm with intact resin tags. C: Composite Resin; A: Adhesive layer; H: Hybrid Layer; Rt: Resin tag; D: Dentin.

3.5. Interfacial observation by TEM and STEM/EDX analysis

Representative TEM images of each group are shown in Fig. 6. Notably, an “SDF-dentin-

reacted layer" was observed on the top of the hybrid layer in all SDF-contaminated dentin groups (Fig. 6g-6l). Further STEM/EDX analysis detected that the primary elements in this layer were calcium and fluoride (Fig. 7). Multiple electron-dense particles, identified as silver, were also found at the top of and within the hybrid layer (Fig. 7a-7e).

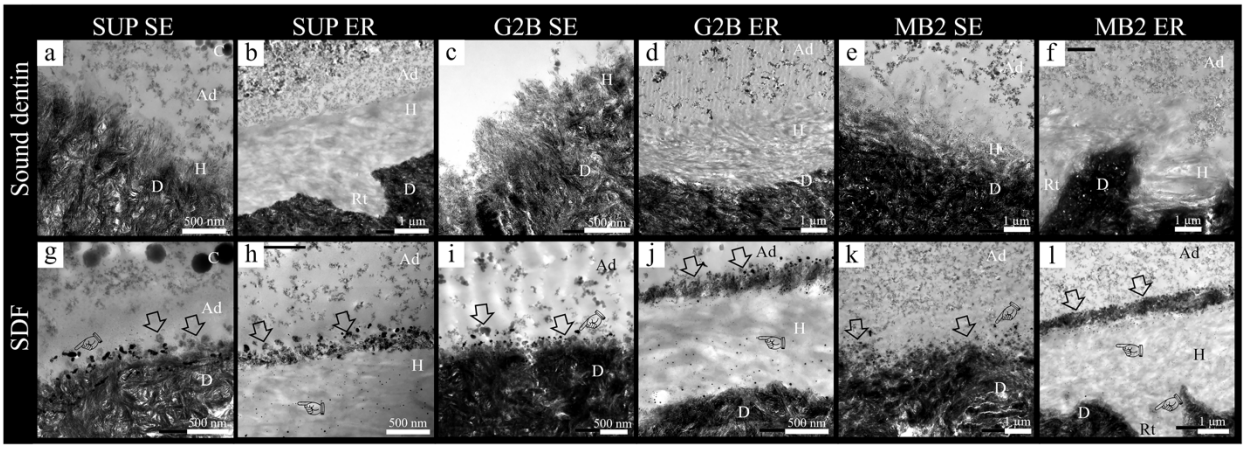

Fig 6. Representative non-demineralized and non-stained TEM images showing ultra-structures of adhesive-dentin interface of each adhesive bonded to sound dentin (**a-f**) and SDF-contaminated dentin (**g-l**). **a:** SUP with SE mode, exhibiting a hybrid layer approximately 200-300 nm thick. **c:** G2B with SE mode, presenting a hybrid layer approximately 400-500 nm thick. **e**: MB2 with SE mode, also presenting a hybrid layer approximately 500 nm thick. **b,d,f**: In all adhesives with ER mode, presenting a tight adhesive-dentin interface with a hybrid layer approximately 2-3 µm thick. **g,i,k**: SDF-contaminated dentin bonded with all adhesives in SE mode, revealing a tight adhesive-dentin interface with a SDF-dentin-reacted layer on top of hybrid layer. Arrow indicates SDF-dentin-reacted layer. **h,j,l**: SDF-contaminated dentin bonded with all adhesives in ER mode, showing a tight adhesive-dentin interface with a hybrid layer approximately 2-3 µm thick, along with a SDF-dentin-reacted layer on top of hybrid layer. Remained small particles were also found within the

hybrid layer. Hand pointer illustrates particles. C: Composite Resin; A: Adhesive Layer; H: Hybrid Layer; Rt: Resin tag; D: Dentin.

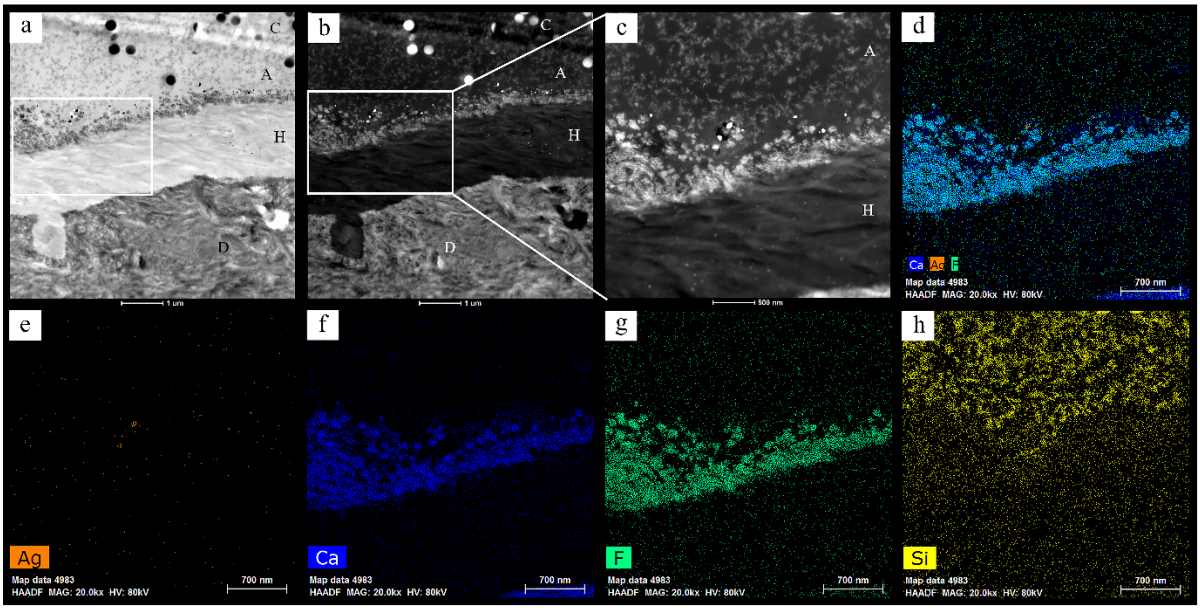

Fig 7. Representative STEM images of SDF-contaminated dentin with SUP in ER mode (**a-c**), along with EDS/STEM element mapping images (**d-h**). **a**: Non-demineralized, non-stained section revealing a tight adhesive-dentin interface with approximately 2-3µm thick hybrid layer. The white box indicates the remaining electron-dense particles on top of and within the hybrid layer. **b-c**: HAADF-STEM image of the same area, presenting the higher atomic numbers in bright areas. **d-h**: EDS/STEM element mapping images of the same area, illustrating each element in the adhesive-interface structure. **d**: overlay of calcium, silver, and fluoride elements. **e**: silver in orange. **f:** calcium in blue. **g**: fluoride in green. **h**: silicon in yellow. C: Composite Resin; A: Adhesive; H: Hybrid Layer; Rt: Resin tag; D: Dentin.

4. Discussion

This study aimed to evaluate the bond strength of SDF-contaminated sound dentin to different adhesives. The results showed the adverse effect of SDF on the dentin bond strength of all adhesives in this study (Fig.1). Therefore, the first null hypothesis was rejected. The reduction in bond strength of SDF-contaminated dentin could be due to several reasons. Firstly, intimate contact is necessary to acquire the adaptation between adhesive and substrate. From our SEM images, the precipitation of silver ions was detected on the dentin surface (Fig. 4b-4c,4e-4f) and occluded the dentinal tubules (Fig. 3e-3h). These silver particles might act as a contaminant on the dentin surface, impeding the resin penetration. Our adhesive-dentin interface observation also supports this statement as the resin tags were scarcely detected in the SDF-contaminated dentin group, especially when SUP (Fig. 5g) and G2B (Fig. 5i) were used in self-etch mode. Moreover, a higher percentage of adhesive failure was observed in the SDF-contaminated group, regardless of the adhesive used (Fig. 2). In addition, the alkaline pH of SDF might buffer the acidic monomer of adhesives tested in this study. The reduction in bond strength of SDF-contaminated dentin was also in agreement with previous studies [27, 28, 40-42].

Additional investigations were conducted on adhesive-dentin interfaces using TEM. Specimens in SDF-contaminated dentin groups presented an “SDF-dentin-reacted layer” on top of the hybrid layer (Fig. 6g-6l). Further analysis with STEM/EDX revealed that this layer primarily consisted of calcium and fluoride (Fig. 7a-7g). This finding is in accordance with an earlier study that demonstrated the presence of calcium and fluoride within sound dentinal tubules [43] and hydroxyapatite [44], which promotes and plays the main role in caries prevention [6, 45, 46]. In addition, silver was also found not only on top of the dentin surface but also within the hybrid layer (Fig. 7a-7e). Future study is necessary to investigate the potential roles of SDF-dentin-reacted

layer, including their chemical formular, long-term apatite formation, and their contribution to caries prevention.

For the etching mode, adhesives applied in ER mode demonstrated significantly higher μTBS than SE mode, except for G2B when bonded to sound dentin (Fig. 1). Therefore, the second null hypothesis was partially rejected. It had been demonstrated in systematic reviews and meta-analyses that the bond strength of universal adhesive to dentin was similar between ER and SE modes [47, 48]. However, the μTBS of SUP and MB2 were significantly lower with SE mode. Most *in vitro* studies reported that the bond strength of Scotchbond Universal, the predecessor of SUP, was not affected by the etching mode [49-53]. Nevertheless, in a 5-year clinical study of class V restoration [54], a significantly lower retention rate was observed when Scotchbond Universal was applied in SE mode (81.4%), compared to those of ER mode (93%) and selective enamel etching (88.4%).

Clearfil SE bond (Clearfil Mega Bond in Japan), the predecessor of MB2, is considered the current gold standard for self-etch adhesive [33]. In this study, we experimentally bonded MB2 with ER mode and showed significantly higher bond strength than SE mode. However, phosphoric acid pretreatment or using MB2 in ER mode was not recommended for dentin bonding [33, 55, 56]. Due to the aggressiveness of phosphoric acid, the dentin was demineralized, exposing a hydroxyapatite-depleted collagen layer, resulting in lower bond strength. Therefore, selective enamel etching was proposed. In contrast, two studies investigated the use of phosphoric acid pretreatment before dentin bonding with 1-step self-etch adhesive, with one study detecting no adverse effect [57] and another study demonstrating higher bond strength on the etched dentin [58] which is similar to the result of MB2 in this study. Therefore, it might be suggested that using MB2 with ER mode is not contraindicated. However, further study is necessary to evaluate the long-

term bond strength of MB2 used in ER mode.

The bond strength in SDF-contaminated dentin was significantly higher when adhesives were applied in ER mode (Fig. 1). This could be due to the high acidity of 35% phosphoric acid which enhanced the bond strength and could partially eliminate the remnants of silver and fluoride on the top of dentin surface (Fig. 3c-3d). This is supported by observations of the adhesive-dentin interface (Fig. 5h, 5j, 5l), where the resin penetration of ER groups appeared similar to those bonded to sound dentin (Fig. 5b, 5d, 5f). This finding is consistent with previous studies that have demonstrated the effect of using acid to remove particles made from SDF or SDF/potassium iodide (KI) which led to the improvement of μTBS [17, 29]. Moreover, the high pH at 10 of SDF could neutralize the acidic monomer of adhesives applied in SE mode and affect bonding performance, as previously mentioned.

Three different 10-MDP-containing adhesives were used in this study. According to the results, there was no significant difference in μTBS among adhesives when bonded in ER mode. However, in SE mode, G2B demonstrated a significantly higher μTBS than SUP. Therefore, the third null hypothesis was rejected. This could be due to the separate bottles of hydrophilic primer and hydrophobic bonding resin of G2B as well as MB2, which was shown to have a more effective influence on bonding to dentin. This hydrophobic layer was proven to inhibit susceptibility to water movement within the adhesive-dentin interface [59, 60]. G2B and MB2 demonstrated a thicker intermediate layer of flexible resin interface that can absorb part of the polymerization shrinkage stress and absorb the shock during function [61, 62] as shown in the SEM image of the adhesive-dentin interface (Fig. 5). G2B is classified as the first 2-step universal adhesive [63]. The G2B primer contains an acidic monomer with a pH of 1.5, which is an intermediate-strong acid that can cause more demineralization of dentin compared to SUP (pH 2.7) and MB2 (pH ~2). In

addition, G2B, without the presence of HEMA, exhibits higher hydrophobicity compared to SUP and MB2, which can be advantageous in terms of reduced water sorption. This known factor can potentially degrade bond durability over time [64]. Nevertheless, further investigation is required to confirm the bond durability of the adhesive interface.

5. Conclusion

Within the limitation of this study, the following conclusion might be drawn.

1. SDF demonstrated an adverse effect on the dentin bond strength of all adhesives. Additionally, ER mode is preferable when bonded to SDF-contaminated dentin.
2. The SDF-dentin-reacted layer, primarily containing calcium and fluoride, was observed.

References

1. Pitts NB, Zero DT, Marsh PD, Ekstrand K, Weintraub JA, Ramos-Gomez F, et al. Dental caries. Nat Rev Di Primers 2017;3:1-16. https://doi.org/10.1038/nrdp.2017.30.

2. Yamaga R. Nishino M, Yoshida S, Yokomizo I. Diamine silver fluoride and its clinical application. J Osaka Univ Dent Sch 1972;12:1-20.

3. Suzuki T, Nishida M, Sobue S, Moriwaki Y. Effects of diammine silver fluoride on tooth enamel. J Osaka Univ Dent Sch 1974;14:61-72.

4. Rosenblatt A, Stamford TCM, Niederman R. Silver diamine fluoride: a caries “silver-fluoride bullet”. J Dent Res. 2009;88:116-25. https://doi.org/10.1177/0022034508329406.

5. Chu CH, Lo ECM, Lin HC. Effectiveness of silver diamine fluoride and sodium fluoride varnish in arresting dentin caries in Chinese pre-school children. J Dent Res 2002;81:767-70. https://doi.org/10.1177/0810767.

6. Mei ML, Nudelman F, Marzec B, Walker JM, Lo ECM, Walls AW, et al. Formation of fluorohydroxyapatite with silver diamine fluoride. J Dent Res 2017;96:1122-8. https://doi.org/10.1177/0022034517709738.

7. Knight GM, McIntyre JM, Craig GG, Zilm PS, Gully NJ. Inability to form a biofilm of Streptococcus mutans on silver fluoride-and potassium iodide-treated demineralized dentin. Quintessence Int 2009;40:155-61.

8. Mei ML, Chu CH, Low KH, Che CM, Lo ECM. Caries arresting effect of silver diamine fluoride on dentine carious lesion with S. mutans and L. acidophilus dual-species cariogenic biofilm. Med Oral Patol Oral Cir Bucal 2013;18:e824-31. https://dx.doi.org/doi:10.4317/medoral.18831.

9. Mei ML, Li QL, Chu CH, Lo ECM, Samaranayake LP. Antibacterial effects of silver diamine

fluoride on multi-species cariogenic biofilm on caries. Ann Clin Microbiol Antimicrob 2013;12:1-7. https://doi.org/10.1186/1476-0711-12-4.

10. FDA U.S. food & drug administration. diammine silver fluoride dental hypersensitivity varnish databases, https://www.accessdata.fda.gov/scripts/cdrh/cfdocs/cfpmn/pmn.cfm?ID=K102973; 2023 [accessed 18 October 2023].

11. Hiraishi N, Sayed M, Takahashi M, Nikaido T, Tagami J. Clinical and primary evidence of silver diamine fluoride on root caries management. Jpn Dent Sci Rev 2022;58:1-8. https://doi.org/10.1016/j.jdsr.2021.11.002.

12. Horst JA. Silver fluoride as a treatment for dental caries. Adv Dent Res 2018;29:135-40. https://doi.org/10.1177/0022034517743750.

13. Horst JA, Ellenikiotis H, Milgrom PL. UCSF protocol for caries arrest using silver diamine fluoride: rationale, indications and consent. J Calif Dent Assoc 2016;44:16-28. https://doi.org/10.1080/19424396.2016.12220962.

14. Llodra JC, Rodriguez A, Ferrer B, Menardia V, Ramos T, Morato M. Efficacy of silver diamine fluoride for caries reduction in primary teeth and first permanent molars of schoolchildren: 36-month clinical trial. J Dent Res 2005;84(8):721-4. https://doi.org/10.1177/154405910508400807.

15. Mei ML, Zhao IS, Ito L, Lo ECM, Chu CH. Prevention of secondary caries by silver diamine fluoride. Int Dent J 2016;66:71-7. https://doi.org/10.1111/idj.12207.

16. Koizumi H, Hamama HH, Burrow MF. Effect of a silver diamine fluoride and potassium iodide-based desensitizing and cavity cleaning agent on bond strength to dentine. Int J Adhes Adhes 2016;68:54-61. https://doi.org/10.1016/j.ijadhadh.2016.02.008.

17. Castillo JL, Rivera S, Aparicio T, Lazo R, Aw TC, Mancl LL, et al. The short-term effects of diammine silver fluoride on tooth sensitivity: a randomized controlled trial. J Dent Res 2011;90:203-8. https://doi.org/10.1177/0022034510388516.

18. Chu CH, Lam A, Lo EC. Dentin hypersensitivity and its management. Gen dent 2011;59:115-22.

19. Chan AKY, Tamrakar M, Jiang CM, Tsang YC, Leung KCM, Chu CH. Effectiveness of 38% silver diamine fluoride in reducing dentine hypersensitivity on exposed root surface in older Chinese adults: study protocol for a randomised double-blind study. Dent J 2022;10:194. https://doi.org/10.3390/dj10100194.

20. Craig GG, Knight GM, McIntyre JM. Clinical evaluation of diamine silver fluoride/potassium iodide as a dentine desensitizing agent. A pilot study. Aust Dent J 2012;57:308-11. https://doi.org/10.1111/j.1834-7819.2012.01700.x.

21. Hiraishi N, Yiu CK, King NM, Tagami J, Tay FR. Antimicrobial efficacy of 3.8% silver diamine fluoride and its effect on root dentin. J Endod 2010;36:1026-9. https://doi.org/10.1016/j.joen.2010.02.029.

22. Sayed M, Nikaido T, Abdou A, Burrow MF, Tagami J. Potential use of silver diammine fluoride in detection of carious dentin. Dent Mater J 2021;40:820-6. https://doi.org/10.4012/dmj.2020-308.

23. Quock RL, Barros JA, Yang SW, Patel SA. Effect of silver diamine fluoride on microtensile bond strength to dentin. Oper Dent 2012;37:610-6. https://doi.org/10.2341/11-344-L.

24. Firouzmandi M, Mohaghegh M, Jafarpisheh M. Effect of silver diamine fluoride on the bond durability of normal and carious dentin. J Clin Exp Dent 2020;12:e468-73. https://doi.org/10.4317/jced.56303.

25. Wu DI, Velamakanni S, Denisson J, Yaman P, Boynton JR, Papagerakis P. Effect of silver diamine fluoride (SDF) application on microtensile bonding strength of dentin in primary teeth. Pediatr Dent 2016;38:148-53.
26. Lutgen P, Chan D, Sadr A. Effects of silver diammine fluoride on bond strength of adhesives to sound dentin. Dent Mater J 2018;37:1003-9. https://doi.org/10.4012/dmj.2017-401.
27. Ko AK, Matsui N, Nakamoto A, Ikeda M, Nikaido T, Burrow MF, et al. Effect of silver diammine fluoride application on dentin bonding performance. Dent Mater J 2020;39:407-14. https://doi.org/10.4012/dmj.2019-057.
28. Uctasli M, Stape THS, Mutluay MM, Tezvergil-Mutluay A. Silver diamine fluoride and resin-dentin bonding: optimization of application protocols. Int J Adhes Adhes 2023;126:e103468. https://doi.org/10.1016/j.ijadhadh.2023.103468.
29. Fröhlich TT, Rocha RDO, Botton G. Does previous application of silver diammine fluoride influence the bond strength of glass ionomer cement and adhesive systems to dentin? Systematic review and meta-analysis. Int J Paediatr Dent 2020;3:85-95. https://doi.org/10.1111/ipd.12571.
30. Jiang M, Mei ML, Wong MCM, Chu CH, Lo ECM. Effect of silver diamine fluoride solution application on the bond strength of dentine to adhesives and to glass ionomer cements: a systematic review. BMC Oral Health 2020;20:e40. https://doi.org/10.1186/s12903-020-1030-z.
31. Van Meerbeek B, Yoshihara K, Van Landuyt K, Yoshida Y, Peumans M. From Buonocore's pioneering acid-etch technique to self-adhering restoratives. A status perspective of rapidly advancing dental adhesive technology. J Adhes Dent 2020;22:7-34. https://doi.org/10.3290/j.jad.a43994.
32. Saikaew P, Sattabanasuk V, Harnirattisai C, Chowdhury AFMA, Carvalho R, Sano H. Role of the smear layer in adhesive dentistry and the clinical applications to improve bonding

performance. Jap Dent Sci Rev 2022;58:59-66. https://doi.org/10.1016/j.jdsr.2021.12.001.

33. Armstrong S, Breschi L, Özcan M, Pfefferkorn F, Ferrari M, Van Meerbeek B. Academy of dental materials guidance on in vitro testing of dental composite bonding effectiveness to dentin/enamel using micro-tensile bond strength (μTBS) approach. Dent Mater 2017;33:133-43. https://doi.org/10.1016/j.dental.2016.11.015.

34. Sano H, Chowdhury AFMA, Saikaew P, Matsumoto M, Hoshika S, Yamauti M. The microtensile bond strength test: its historical background and application to bond testing. Jap Dent Sci Rev 2020;56:24-31. https://doi.org/10.1016/j.jdsr.2019.10.001.

35. Perdigao J, Lambrechts P, Van Meerbeek B, Vanherle G, Lopes ALB. Field emission SEM comparison of four postfixation drying techniques for human dentin. J Biomed Mater Res 1995;29:1111-20. https://doi.org/10.1002/jbm.820290911.

36. Yuan Y, Intajak P, Islam R, Ting S, Matsumoto M, Hoshika S, et al. Effect of sodium hypochlorite on bonding performance of universal adhesives to pulp chamber dentin. J Dent Sci 2023;18:1116-24. https://doi.org/10.1016/j.jds.2022.11.007.

37. Van Meerbeek B, Yoshida Y, Lambrechts P, Vanherle G, Duke ES, Eick JD, et al. A TEM study of two water-based adhesive systems bonded to dry and wet dentin. J Dent Res 1998;77:50-9. https://doi.org/10.1177/00220345980770010501.

38. Hoshika S, Ting S, Ahmed Z, Chen F, Toida Y, Sakaguchi N, et al. Effect of conditioning and 1 year aging on the bond strength and interfacial morphology of glass-ionomer cement bonded to dentin. Dent Mater 2021;37:106-12. https://doi.org/10.1016/j.dental.2020.10.016.

39. Knight GM, McIntyre JM, Mulyani. The effect of silver fluoride and potassium iodide on the bond strength of auto cure glass ionomer cement to dentine. Aust Dent J 2006;51:42-5. https://doi.org/10.1111/j.1834-7819.2006.tb00399.x.

40. Frohlich TT, Botton G, Rocha RDO. Bonding of glass-ionomer cement and adhesives to silver diamine fluoride-treated dentin: an updated systematic review and meta-analysis. J Adhes Dent 2022;24:29-38. https://doi.org/10.3290/j.jad.b2701679.

41. Markham MD, Tsujimoto A, Barkmeier WW, Jurado CA, Fischer NG, Watanabe H, et al. Influence of 38% silver diamine fluoride application on bond stability to enamel and dentin using universal adhesives in self-etch mode. Eur J Oral Sci 2020;128:354-60. https://doi.org/10.1111/eos.12701.

42. Sayed M, Matsui N, Uo M, Nikaido T, Oikawa M, Burrow MF, et al. Morphological and elemental analysis of silver penetration into sound/demineralized dentin after SDF application. Dent Mater 2019;35:1718-27. https://doi.org/10.1016/j.dental.2019.08.111.

43. Yu OY, Mei ML, Zhao IS, Li QL, Lo ECM, Chu CH. Remineralisation of enamel with silver diamine fluoride and sodium fluoride. Dent Mater 2018;34:e344-52. https://doi.org/10.1016/j.dental.2018.10.007.

44. Lou YL, Botelho MG, Darvell BW. Reaction of silver diamine fluoride with hydroxyapatite and protein. J Dent 2011;39:612-8. https://doi.org/10.1016/j.jdent.2011.06.008.

45. Yamaga R, Nishino M, Yoshida S, Yokomizo I. Diammine silver fluoride and its clinical application. J Osaka Univ Dent Sch 1972;12:1-20.

46. Hiraishi N, Sayed M, Hill R, Shimada Y. Solid-state NMR spectroscopy measurement of fluoride reaction by bovine enamel and dentin treated with silver diammine fluoride. Dent Mater 2022;38:769-77. https://doi.org/10.1016/j.dental.2022.04.017.

47. Da Rosa WL, Piva E, Da Silva AF. Bond strength of universal adhesives: a systematic review and meta-analysis. J Dent 2015;43:765-76. https://doi.org/10.1016/j.jdent.2015.04.003.

48. Chen H, Feng S, Jin Y, Hou Y, Zhu S. Comparison of bond strength of universal adhesives

using different etching modes: a systematic review and meta-analysis. Dent Mater J 2022;41:1-10. https://doi.org/10.4012/dmj.2021-111.

49. Muñoz MA, Luque I, Hass V, Reis A, Loguercio AD, Bombarda NHC. Immediate bonding properties of universal adhesives to dentine. J Dent 2013;41:404-11. https://doi.org/10.1016/j.jdent.2013.03.001.

50. Sezinando A, Luque-Martinez I, Muñoz MA, Reis A, Loguercio AD, Perdigão J. Influence of a hydrophobic resin coating on the immediate and 6-month dentin bonding of three universal adhesives. Dent Mater 2015;31:e236-46. https://doi.org/10.1016/j.dental.2015.07.002.

51. Yamauchi K, Tsujimoto A, Jurado CA, Shimatani Y, Nagura Y, Takamizawa T, et al. Etch-and-rinse vs self-etch mode for dentin bonding effectiveness of universal adhesives. J Oral Sci 2019;61:549-53. https://doi.org/10.2334/josnusd.18-0433.

52. Wagner A, Wendler M, Petschelt A, Belli R, Lohbauer U. Bonding performance of universal adhesives in different etching modes. J Dent 2014;42:800-7. https://doi.org/10.1016/j.jdent.2014.04.012.

53. Chen C, Niu LN, Xie H, Zhang ZY, Zhou LQ, Jiao K, et al. Bonding of universal adhesives to dentine – Old wine in new bottles?. J Dent 2015;43:525-36. https://doi.org/10.1016/j.jdent.2015.03.004.

54. de Paris Matos T, Perdigão J, de Paula E, Coppla F, Hass V, Scheffer RF, et al. Five-year clinical evaluation of a universal adhesive: a randomized double-blind trial. Dent Mater 2020;36:1474-85. https://doi.org/10.1016/j.dental.2020.08.007.

55. Van Landuyt KL, Peumans M, Munck JD, Lambrechts P, Van Meerbeek B. Extension of a one-step self-etch adhesive into a multi-step adhesive. Dent Mater 2006;22:533-44. https://doi.org/10.1016/j.dental.2005.05.010.

56. Buonocore MG. A simple method of increasing the adhesion of acrylic filling materials to enamel surfaces. J Dent Res 1955;34:849-53. https://doi.org/10.1177/00220345550340060801.

57. Proença JP, Polido M, Osorio E, Erhardt MCG, Aguilera FS, García-Godoy F, et al. Dentin regional bond strength of self-etch and total-etch adhesive systems. Dent Mater 2007;23:1542-8. https://doi.org/10.1016/j.dental.2007.02.001.

58. Taschner M, Nato F, Mazzoni A, Frankenberger R, Krämer N, Di Lenarda R, et al. Role of preliminary etching for one-step self-etch adhesives. Eur J Oral Sci 2010;118:517-24. https://doi.org/10.1111/j.1600-0722.2010.00769.x.

59. Yamanaka A, Mine A, Matsumoto M, Hagino R, Yumitate M, Ban S, et al. Back to the multi-step adhesive system: a next-generation two-step system with hydrophobic bonding agent improves bonding effectiveness. Dent Mater J 2021;40:928-33. https://doi.org/10.4012/dmj.2020-272.

60. Sukprasert N, Harnirattisai C, Senawongse P, Sano H, Saikaew P. Delayed light activation of resin composite affects the bond strength of adhesives under dynamic simulated pulpal pressure. Clin Oral Investig 2022;26:6743-52. https://doi.org/10.1007/s00784-022-04634-3.

61. De Munck J, Van Landuyt KL, Coutinho E, Poitevin A, Peumans M, Lambrechts P, et al. Fatigue resistance of dentin/composite interfaces with an additional intermediate elastic layer. Eur J Oral Sci 2005;113:77-82. https://doi.org/10.1111/j.1600-0722.2004.00185.x.

62. Chowdhury AFMA, Alam A, Yamauti M, Alvarez Lloret P, Saikaew P, Carvalho RM, et al. Characterization of an experimental two-step self-stch adhesive's bonding performance and resin-dentin interfacial properties. Polymers (Basel) 2021;13:e1009. https://doi.org/10.3390/polym13071009.

63. The new standard in adhesive dentistry. Br Dent J. 2021;230:263.

https://doi.org/10.1038/s41415-021-2719-3

64. Takahashi M, Nakajima M, Hosaka K, Ikeda M, Foxton RM, Tagami J. Long-term evaluation of water sorption and ultimate tensile strength of HEMA-containing/-free one-step self-etch adhesives. J Dent 2011;39:506-12. https://doi.org/10.1016/j.jdent.2011.04.008.